Inorg. Chem. **2006**, *45*, 8009–8011

Electrochemical Generation of a Nonheme Oxoiron(IV) Complex

Michael J. Collins,[†,‡] Kallol Ray,[†] and Lawrence Que, Jr.*[,†]

Department of Chemistry and Center for Metals in Biocatalysis, University of Minnesota, 207 Pleasant Street SE, Minneapolis, Minnesota 55455, and Chemistry Department, Viterbo University, La Crosse, Wisconsin 54601

Received July 7, 2006

The complex $[Fe^{IV}O(N4Py)]^{2+}$ (N4Py = *N*,*N*-bis(2-pyridylmethyl)-*N*-bis(2-pyridyl)methylamine) has been prepared by bulk electrolysis in aqueous CH_3CN and CH_2Cl_2, and its redox properties characterized. Bulk chronocoulometry and spectropotentiometry experiments in CH_3CN show that $[Fe^{II}(N4Py)(NCCH_3)]^{2+}$ can be oxidized quantitatively to its iron(III) derivative at an applied potential of +0.71 V vs ferrocene and then to the oxoiron(IV) complex (in the presence of added water) at potentials above +1.3 V. The $E_{1/2}$ value for the $Fe^{IV/III}$ couple has been estimated to be +0.90 V from spectropotentiometric titrations in CH_3CN and cyclic voltammetric measurements in CH_2Cl_2.

In the past few years, a number of mononuclear complexes with oxoiron(IV) units supported by polydentate nonheme ligands have been characterized.[1] These complexes serve as models for high-valent intermediates in the catalytic cycles of nonheme iron enzymes that carry out a range of oxidative transformations.[2] One such intermediate has been identified as the oxidant in taurine: α-ketoglutarate dioxygenase.[3] Several of the biomimetic nonheme iron−oxo complexes have been isolated and structurally characterized by X-ray crystallography,[4a,b] and by Fe K-edge X-ray absorption spectroscopy,[4c] thereby providing a structural basis for the interpretation of their spectroscopic properties. These oxoiron(IV) complexes have been shown to carry out a number of substrate oxidations,[4a,5] including the hydroxylation of cyclohexane by $[Fe^{IV}O(N4Py)]^{2+}$ (**3**)[5a] [N4Py = *N*,*N*-bis(2-pyridylmethyl)-*N*-bis(2-pyridyl)methylamine)], suggesting that these complexes can be powerful oxidants.[6] To date, no detailed electrochemical study has been reported on any of the above nonheme oxoiron(IV) complexes that provides a rationale for their oxidative reactivity.[7] Our initial investigations have focused on the electrochemistry of $[Fe^{II}(N4Py)(NCMe)](OTf)_2$ (**1a**$(OTf)_2$)[4c] and its oxoiron(IV) derivative **3** because of the latter's significant thermal stability. In this paper, we report the electrochemical generation of **3** from **1a** and the determination of its $Fe^{IV/III}$ potential.

Scheme 1. Redox Chemistry of Fe(N4Py) Species

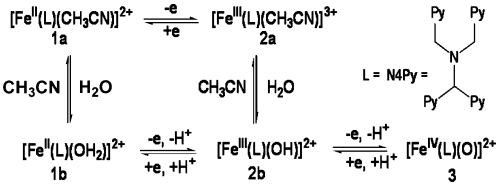

The redox chemistry of Fe(N4Py) can be thought of as a series of one-electron reactions traversing from the iron(II) starting point **1a** via iron(III) species **2a** and **2b** to **3** (Scheme 1). As reported previously[8] and shown in Figure 1a, cyclic voltammetry (CV) experiments with a glassy carbon microelectrode show that **1a** undergoes a quasi-reversible one-electron oxidation in CH_3CN solvent at +0.61 V associated with the **2a**/**1a** couple (all potentials reported relative to the

* To whom correspondence should be addressed. E-mail: que@chem.umn.edu.
† University of Minnesota.
‡ Viterbo University.

(1) Shan, X.; Que, L., Jr. *J. Inorg. Biochem.* **2006**, *100*, 421−433.
(2) (a) Costas, M.; Mehn, M. P.; Jensen, M. P.; Que, L., Jr. *Chem. Rev.* **2004**, *104*, 939−986. (b) Abu-Omar, M. M.; Loaiza, A.; Hontzeas, N. *Chem. Rev.* **2005**, *105*, 2227−2252.
(3) (a) Bollinger, J. M., Jr.; Price, J. C.; Hoffart, L. M.; Barr, E. W.; Krebs, C. *Eur. J. Inorg. Chem.* **2005**, 4245−4254. (b) Krebs, C.; Price, J. C.; Baldwin, J.; Saleh, L.; Green, M. T.; Bollinger, J. M., Jr. *Inorg. Chem.* **2005**, *44*, 742−757.
(4) (a) Rohde, J.-U.; In, J.-H.; Lim, M. H.; Brennessel, W. W.; Bukowski, M. R.; Stubna, A.; Münck, E.; Nam, W.; Que, L., Jr. *Science* **2003**, *299*, 1037−1039. (b) Klinker, E. J.; Kaizer, J.; Brennessel, W, W.; Woodrum, N. L.; Cramer, C. J.; Que, L., Jr. *Angew. Chem., Int. Ed.* **2005**, *44*, 3690−3694. (c) Rohde, J.-U.; Torelli, S.; Shan, X.; Lim, M. H.; Klinker, E. J.; Kaizer, J.; Chen, K.; Nam, W.; Que, L., Jr. *J. Am. Chem. Soc*, **2004**, *126*, 16750−16761.
(5) (a) Kaizer, J.; Klinker, E. J.; Oh, N. Y.; Rohde, J.-U.; Song, W. J.; Stubna, A.; Kim, J.; Münck, E.; Nam, W.; Que, L., Jr. *J. Am. Chem. Soc.* **2004**, *126*, 472−473. (b) Lim, M. H.; Rohde, J.-U.; Stubna, A.; Bukowski, M. R.; Costas, M.; Ho, R. Y. N.; Münck, E.; Nam, W.; Que, L., Jr. *Proc. Natl. Acad. Sci. U.S.A.*, **2003**, *100*, 3665−3670. (c) Oh, N. Y.; Suh, Y.; Park, M. J.; Seo, M. S.; Kim, J.; Nam, W. *Angew. Chem., Int. Ed.* **2005**, *44*, 4235−4239. (d) Paine, T. K.; Costas, M.; Kaizer, J.; Que, L., Jr. *J. Biol. Inorg. Chem.* **2006**, *11*, 272−276.
(6) (a) Kumar, D.; Hirao, H.; Que, L., Jr.; Shaik, S. *J. Am. Chem. Soc.* **2005**, *127*, 8026−8027. (b) Hirao, H.; Kumar, D.; Que, L., Jr.; Shaik, S. *J. Am. Chem. Soc.* **2006**, *128*, 8590−8606.
(7) Sastri, C. V.; Oh, K.; Lee, Y. J.; Seo, M. S.; Shin, W.; Nam, W. *Angew. Chem. Int. Ed.* **2006**, *45*, 3992−3995.
(8) (a) Roelfes, G.; Lubben, M.; Chen, K.; Ho, R. Y. N.; Meetsma, A.; Genseberger, S.; Hermant, R. M.; Hage, R.; Mandal, S. K.; Young, V. G., Jr.; Zang, Y.; Kooijman, H.; Spek, A. L.; Que, L., Jr.; Feringa, B. L. *Inorg. Chem.* **1999**, *38*, 1929−1936. (b) Roelfes, G.; Vrajmasu, V.; Chen, K.; Ho, R. Y. N.; Rohde, J.-U.; Zondervan, U.; la Crois, R. M.; Schudde, E. P.; Lutz, M.; Spek, A. L.; Hage, R.; Feringa, B. L.; Münck, E.; Que, L., Jr. *Inorg. Chem.* **2003**, *42*, 2639−2653.

10.1021/ic061263i CCC: $33.50
Published on Web 09/06/2006

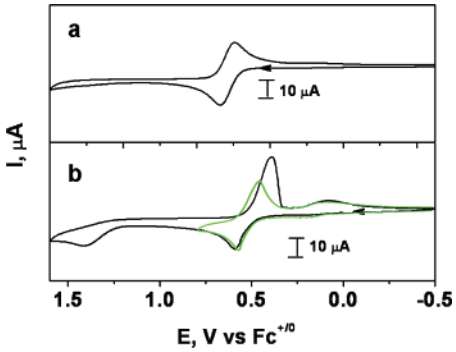

Figure 1. Cyclic voltammetry of **1a** in (a) CH_3CN and (b) CH_2Cl_2 at 25 °C (0.1 M NBu_4BF_4 supporting electrolyte, glassy carbon working and platinum auxiliary electrodes; scan rate of 0.2 V s^{-1}). Potentials are vs the $Fc^{+/0}$ couple, and the arrow indicates the direction of scans.

ferrocinium/ferrocene couple, $Fc^{+/0}$). Scanning anodically up to +1.6 V does not elicit another feature corresponding to a further oxidation to form **3**. Since formation of **3** may be prevented by the lack of an oxygen-atom source, additional CV experiments were carried out in the presence of added water (Figures S1 and S2). Indeed addition of water elicits the appearance of a new reduction wave at $E_{p,c}$ = +0.15 V that intensifies with increased water concentration at the expense of the wave at +0.61 V. This feature is assigned to the $Fe^{III/II}$ couple of $[Fe^{II}(N4Py)(OH_2)]^{2+}$ (**1b**) and becomes more evident in the return scan after **1a** undergoes oxidation, suggesting the more facile displacement of CH_3CN from **1a** by water upon oxidation to **2a**. Even under these 'wet' conditions, CV experiments at higher potential did not elicit a feature that can be assigned to the formation of **3**, suggesting that either the incorrect potential range was being monitored or that there is a kinetic barrier to the oxidation.

As an alternative strategy, controlled potential bulk electrolysis experiments using a large-surface-area reticulated vitreous carbon electrode (see Supporting Information for details) were carried out on **1a** in CH_3CN. Application of a potential of +0.71 V, sufficient to oxidize >99% of **1a** by one electron, based on the $E_{1/2}$ value of +0.61 V, elicited within 20 min the conversion of the amber color characteristic of **1a** to a lemon yellow solution. The initial amber color could be restored upon switching the potential to 0.0 V. The lemon yellow species exhibits a UV shoulder at about 300−320 nm that is assigned to $[Fe^{III}(N4Py)(OH)]^{2+}$ (**2b**), which could be independently prepared by the addition of 0.5 equiv of H_2O_2 to **1a**.[8a] These observations support a reaction sequence in which **1a** is first oxidized to **2a**, which is in turn converted to **2b** in a ligand exchange step promoted by the added water.

Electrolysis at ≥ +1.3 V resulted in the much slower conversion of the lemon yellow solution to a pale blue-green solution (see Supporing Information for details). The UV−vis spectrum of the blue-green solution gave an absorbance maximum and a molar absorbance identical to those reported earlier[5a] for **3** (vide infra). Switching from a high poising potential to 0.0 V resulted in the rapid reduction of **3** back to **1a**.

As a further substantiation of the redox chemistry, spectroelectrochemistry experiments were carried out to monitor

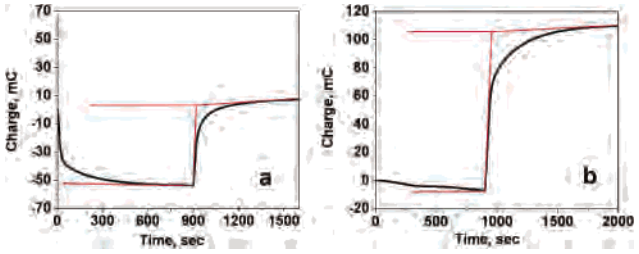

Figure 2. Spectrochronocoulometry of **1a** (2.30 mL of a 0.27 mM solution in CH_3CN containing 0.1 M H_2O and 0.1 M NBu_4BF_4 as supporting electrolyte at 20 °C). (a) Oxidizing jump from −0.20 to +0.71 V, followed by a reducing jump to −0.20 V; charges passed were −52 and +54 mC, respectively. (b) Reducing jump from +1.3 to +0.71 V, followed by a jump to −0.20 V; charges passed were −7 and +118 mC, respectively.

the spectral changes associated with **1a**, **2b**, and **3** as a function of the applied potential. Controlled potential spectrochronocoulometry from an initial poise of −0.20 V jumped to +0.71 V showed a complete loss, over a 15−20 min period, of the 455- and 380-nm bands associated with **1a**. Currents peaked at about 1 mA and declined to less than 10 μA over this time period. Subsequent reduction back to **1a** was rapid and quantitative. Chronocoulometry gave within 5% of the expected number of coulombs for a one-electron redox reaction (Figure 2a). Subsequent jumps to +1.4 V gave complete conversion to **3** within 30 min, based on the appearance of its characteristic 695-nm absorption band.[5a] Initial currents again were in the 1 mA range, but the residual oxidizing current was much higher at +1.4 V, about 50 μA, due to competing oxidation of the added water (Figure S2). As a result, chronocoulometry gave about 30% more millicoulombs than would be expected for a one-electron oxidation. In all cases, the return jump from +1.4 to +0.71 V elicited no reducing current nor spectral changes over 20 min or more. However, a jump from +0.71 to −0.20 V initiated immediate spectral changes and large reducing currents (Figure 2b), eventually restoring the initial spectrum of **1a**. These results show that **1a** in CH_3CN can be oxidized to **3** in two one-electron steps, but reduction of **3** is a two-electron process.

The rate of formation of **3** at +1.3 V increased with increasing concentration of added water. Electrolysis at higher potentials, up to +2 V, also increased the rate of formation of **3**. Thus, the rate of electrolytic formation of **3** is a function of the applied potential, the working electrode surface area relative to cell volume, and the concentration of added H_2O. The absence of a **2b**/**3** oxidation wave in the CV experiment can thus be attributed to the small surface area of the microelectrode and the low concentration of **2b** formed at the electrode surface. As will be presented below, a switch from CH_3CN to CH_2Cl_2 allows the **2b**/**3** oxidation wave to be observed by CV (Figure 1b).

A spectropotentiometric titration was carried out in CH_3CN with 1 M H_2O to estimate the midpoint potential of the irreversible formation of **3** from **2.** The conversion of **1** to **2** was essentially complete under these conditions with the application of a +0.71 V potential, and **3** began to form only above this potential. Difference spectra vs the spectrum obtained at +0.71 V were computed and representative spectra are shown in Figure 3. The changes in absorbance

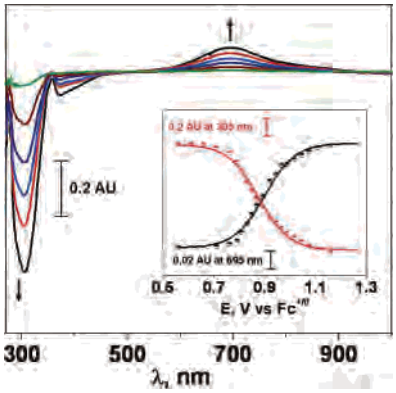

Figure 3. Representative difference spectra relative to the spectrum at 0.71 V in the spectropotentiometric titration of 0.2 mM **2b** to form **3** in CH_3CN at 20 °C. The inset shows the plot of ΔA vs potential for the respective bands at 695 and 305 nm. AU = absorbance units.

at 305 and 695 nm for all difference spectra are shown in the inset. The solid line in each case is the line computed from a fit to the Nernst equation[9] (see Supporting Information for further details). The best fit at 695 nm gave $\Delta\epsilon = 0.38$ mM^{-1} cm^{-1} and a midpoint oxidation potential ($E_{1/2}$) of +0.90 V, while the fit at 305 nm gave $E_{1/2} = +0.88$ V, with $\Delta\epsilon = -3.25$ mM^{-1} cm^{-1}.

Analogous experiments carried out in CH_2Cl_2 corroborate the results obtained in CH_3CN and enhance our understanding of the redox chemistry of **3**. Figure 1b (green line) shows the cyclic voltammogram of **1a** in CH_2Cl_2 with a quasi-reversible wave for the **1a**/**2a** couple at +0.58 V, provided that the CV scan does not go beyond +0.8 V. The Fe^{III}/Fe^{II} reduction wave assigned to **1b** is also present in CH_2Cl_2 at +0.15 V and becomes more evident in the return scan after **1a** undergoes oxidation when residual water is present in the solvent. This wave is more intense in CH_2Cl_2 than in CH_3CN, indicating a higher concentration of **2b** in CH_2Cl_2 upon oxidation of **1a**, as expected for a mass action effect on the **2a**/**2b** equilibrium.

An irreversible oxidative wave appears at +1.4 V (i_a = 11 μA) upon scanning above +0.8 V in CH_2Cl_2, which is notably absent in CH_3CN (Figure 1); this feature is observed only when trace water is present in the solvent. On the reverse scan, there is a dramatic change in the appearance of the reducing wave near +0.4 V, with a near doubling of the reducing current (Figure 1b, black line; i_c = 20 μA). Spectroelectrochemistry in CH_2Cl_2 at 5 °C shows quantitative conversion of **2b** to **3** between 1.1 and 1.4 V (Figure S3), with a visible spectrum virtually identical to that obtained in CH_3CN. Moreover, **3** can be quantitatively reduced back to **2b**, which is not possible in CH_3CN. It is thus reasonable to assign the oxidative wave at +1.4 V ($E_{p,a}$) to the oxidation of **2b** to **3** in CH_2Cl_2 and its reduction to the wave at +0.4 V ($E_{p,c}$).The absence of a similar feature in CH_3CN suggests that the rate of electrochemical formation of **3** is much slower in CH_3CN than in CH_2Cl_2 and further corroborates the notion that the substitution of CH_3CN in **2a** by hydroxide to form **2b** must occur for **3** to be formed (Scheme 1). The slower ligand exchange in CH_3CN makes the formation of **3** kinetically too hindered to be directly observed by CV in CH_3CN, in contrast to the results obtained in CH_2Cl_2.

The large potential difference (ΔE = 1 V) between the oxidizing and reducing peaks associated with **3** in CH_2Cl_2 is similar to those observed for $[(L)_2Fe^{III}{}_2(O)(OAc)_2]^{n+}$ (L = tridentate N3 ligand) complexes,[10] reflecting very slow electron transfer at the working electrode. We speculate that the kinetic barrier to the reduction of the Fe^{IV} species may be due to converting an $S = 1$ Fe^{IV} center to an $S = 5/2$ Fe^{III} center. From the CV data in CH_2Cl_2, the $E_{1/2}$ value for the **2b**/**3** couple can be estimated to be +0.90 V by using the relation $E_{1/2} = (E_{p,a} + E_{p,c})/2$,[10] in good agreement with the spectropotentiometric results in CH_3CN.

Within the context of the limited database of Fe^{IV}/Fe^{III} couples ranging from 1.2 to −0.3 V vs $Fc^{+/0}$, the redox potential of **3** falls at the high end of these values, comparable to those measured for $[(L)_2Fe^{III}{}_2(O)(OAc)_2]^{n+}$ complexes[10] but 0.3−1.1 V higher than for the values found for complexes of dianionic porphyrin,[11b] trianionic ureaylate,[11c] and tetraanionic amidate ligands.[11c] Our value for **3** differs significantly from the $E_{p,c}$ value of −0.44 V observed by Sastri et al.[7] in the cyclic voltammetry of chemically produced **3** in CH_3CN. In our view, the latter negative value reflects not the true reduction potential of **3**, but instead the large kinetic barrier associated with its reduction,[10] particularly in the absence of protons needed to form **2b**. The redox potential for **3**, determined in our experiments from spectropotentiometric titrations in wet CH_3CN and cyclic voltammetric experiments in wet CH_2Cl_2, is much more positive ($E_{1/2}$ = +0.9 V vs $Fc^{+/0}$). In light of Mayer's work,[12] the high potential of **3** provides a strong rationale for its observed ability to oxidize hydrocarbons, including cyclohexane.[5a]

Acknowledgment. This work was supported by the National Science Foundation (CHE0113894, M.J.C.) and the National Institutes of Health (GM-33162, L.Q.). We are grateful to Mr. Sang-Mok Lee for the synthesis of **1a**.

Supporting Information Available: Experimental procedures, the CV of **1a** in dry and wet CH_3CN (Figure S1), the solvent windows for the CV experiments in 'dry' and 'wet' solvents (Figure S2), and the spectroelectrochemistry of **1a** in CH_2Cl_2 (Figure S3). This material is available free of charge via the Internet at http://pubs.acs.org.

IC061263I

(9) Arciero, D. M.; Collins, M. J.; Haladjian, J.; Bianco, P.; Hooper, A. B. *Biochemistry* **1991**, *30*, 11459−11465.

(10) Slep, L. D.; Mijovilovich, A.; Meyer-Klaucke, W.; Weyhermuller, T.; Bill, E.; Bothe, E.; Neese, F.; Wieghardt, K. *J. Am. Chem. Soc.* **2003**, *125*, 15554−15570.

(11) (a) Lee, W. A.; Calderwood, T. S.; Bruice, T. C. *Proc. Natl. Acad. Sci. U.S.A.* **1985**, *82*, 4301−4305. (b) Groves, J. T.; Gross, Z.; Stern, M. K. *Inorg. Chem.* **1994**, *33*, 5065−5072. (c) Gupta, R.; Borovik, A. S. *J. Am. Chem. Soc.* **2003**, *125*, 13234−13242. (d) Ghosh, A.; Tiago de Oliveira, F.; Yano, T.; Nishioka, T.; Beach, E. S.; Kinoshita, I.; Münck, E.; Ryabov, A. D.; Horwitz, C. P.; Collins, T. J. *J. Am. Chem. Soc.* **2005**, *127*, 2505−2513.

(12) Mayer, J. M. *Acc. Chem. Res.* **1998**, *31*, 441−450.